

# 1 **MINOTAUR: A platform for the analysis and visualization of multivariate** 2 **results from genome scans with R Shiny**

3 Robert Verity\*<sup>1§</sup>, Caitlin Collins\*<sup>1</sup>, Daren C. Card<sup>2</sup>, Sara M. Schaal<sup>3</sup>, Liuyang Wang<sup>4</sup>, Katie E.  
4 Lotterhos<sup>3</sup>

5 *\* These authors contributed equally to this work.*

6 <sup>1</sup>Imperial College London, MRC Centre for Outbreak Analysis and Modelling, Department of  
7 Infectious Disease Epidemiology, St. Mary's Campus, Norfolk Place, Imperial College  
8 London, London W21PG, UK

9 <sup>2</sup>Department of Biology, 501 S. Nedderman Drive, The University of Texas at Arlington,  
10 Arlington, TX 76019, USA

11 <sup>3</sup>Department of Marine and Environmental Sciences, 430 Nahant Road, Northeastern  
12 University, Nahant, MA 01908, USA

13 <sup>4</sup>Department of Molecular Genetics and Microbiology, School of Medicine, 213 Research  
14 Drive, Duke University, Durham, NC 27710, USA

15

16 <sup>§</sup>**Correspondence:** [r.verity@imperial.ac.uk](mailto:r.verity@imperial.ac.uk)

17 **Running Head:** Multivariate outliers in genomics

## 18 **Abstract**

19 Genome scans are widely used to identify “outliers” in genomic data: loci with different  
20 patterns compared with the rest of the genome due to the action of selection or other  
21 non-adaptive forces of evolution. These genomic datasets are often high-dimensional,  
22 with complex correlation structures among variables, making it a challenge to identify  
23 outliers in a robust way. The Mahalanobis distance has been widely used for this  
24 purpose, but has the major limitation of assuming that data follow a simple parametric  
25 distribution. Here we develop three new metrics that can be used to identify outliers in  
26 multivariate space, while making no strong assumptions about the distribution of the  
27 data. These metrics are implemented in the R package MINOTAUR, which also includes

28 an interactive web-based application for visualizing outliers in high-dimensional  
29 datasets. We illustrate how these metrics can be used to identify outliers from  
30 simulated genetic data, and discuss some of the limitations they may face in application.

31 **Keywords:** genomic scans, Mahalanobis, kernel density

## 32 **Introduction**

33 Knowledge of the genetic architecture of biological traits—the number of loci that  
34 affect a phenotype, the magnitude of their effect, and their distribution across the  
35 genome—not only illuminates the evolutionary processes that shape genomes, but also  
36 has important implications for complex diseases (McCarthy and Hirschhorn 2008),  
37 conservation (Kohn et al. 2006; Allendorf et al. 2010; Funk et al. 2012), and breeding  
38 programs (Goddard et al. 2009; Varshney et al. 2009). With the advent of next-  
39 generation sequencing we now have the ability to examine genomes at a fine scale; and,  
40 as a result, we have identified a large number of genomic variants that are implicated in  
41 complex diseases (Carlson et al. 2004; Hindorff et al. 2009) and adaptation to the local  
42 environment (Savolainen et al. 2013). This wealth of data is likely to yield new insights,  
43 but it also brings with it the challenge of extracting the relevant signal from noisy,  
44 complex, multi-dimensional data sets. This is perhaps one reason why most of the  
45 variants detected so far have only managed to explain a very small proportion of the  
46 observable phenotypic variation (Yang et al. 2010; Brachi et al. 2011).

47 The preferred method for detecting genomic variants is via genome scans. There are  
48 many different approaches toward scanning genomes, but all are based on the same  
49 premise: that the loci of interest to the investigator are likely to be statistical outliers  
50 when compared with the rest of the genome. The particular choice of statistic will

51 depend on the question being asked and the experimental design, and may include one  
52 or more statistics from the following categories: tests for genetic differentiation  
53 (Lotterhos & Whitlock 2014; Hoban et al. *in revision*), scans for strong positive selection  
54 and/or selective sweeps (Hohenlohe 2010; Vatsiou et al. 2016), genome-wide  
55 association studies for phenotype-associated loci (GWAS, reviewed in Carlson et al.  
56 2004 and McCarthy et al. 2008), linkage mapping for quantitative trait loci (QTL,  
57 Savolainen et al. 2013), genetic-environment associations (reviewed in Rellstab et al.  
58 2015), and scans for differentially expressed genes (Wang et al. 2009). A number of  
59 different genome-scan test statistics may be calculated for a single genomic dataset and  
60 these are usually examined one-at-a-time (i.e., in univariate analyses). Some test  
61 statistics may be highly correlated, while the power of other test statistics may vary for  
62 different regions of the genome depending on the details of selection, recombination,  
63 mutation, and migration rates (Tiffin and Ross-Ibarra 2014). Additionally, the power of  
64 different approaches may vary among species because of demographic history, and  
65 within a species because of sampling design (De Mita et al. 2013; de Villemereuil et al.  
66 2014; Lotterhos and Whitlock 2015). Finally, loci with intermediate probabilities of  
67 detection will often exhibit the highest variance in results from genome scans  
68 (Lotterhos et al. *in review*).

69 Given the complex evolutionary histories of most species, it is doubtful whether any  
70 single statistic can fully capture the genomic signal of interest in the majority of cases  
71 (Verity and Nichols 2014). Furthermore, the uncertainty in demographic history,  
72 coupled with the variation in statistical outcomes in different scenarios, makes it  
73 difficult to know which statistics have the greatest power to detect selection and which

74 have the highest false positive rates. These issues point to a need for composite,  
75 multivariate outlier methods that integrate information across multiple test statistics.

76 Multivariate methods have been utilized extensively in many biological applications,  
77 although in application to genome scans the power of the multivariate approach for  
78 detecting outliers has not yet been fully evaluated. Because some dimension reduction  
79 methods such as Principal Component Analysis rely on assumptions about the data that  
80 may be unjustifiable in the context of genome scans (O'reilly et al. 2012), these methods  
81 are not ideally designed for the identification of multivariate outliers (Patterson et al.  
82 2006). Some GWAS analyses have successfully employed multivariate approaches to  
83 identify genetic associations with multiple phenotypes (O'reilly et al. 2012; Galesloot et  
84 al. 2014). Additionally, multivariate approaches have also been used in GWAS meta-  
85 analysis to simultaneously consider multiple genetic or phenotypic variables (reviewed  
86 in Evangelou and Ioannidis 2013). It is evident, however, that more opportunities exist  
87 for the use of multivariate approaches in outlier detection than are currently being  
88 capitalized on.

89 While there are dedicated software tools for calculating a variety of test statistics, there  
90 does not currently exist a unified platform for the filtering, visualization, and integration  
91 of test statistics in multivariate space. Here we describe a new R package called  
92 MINOTAUR (Multivariate visualisation and Outlier Analysis Using R) built specifically  
93 for this purpose. This software package - initiated during a hackathon for population  
94 genetics in R (<https://github.com/NESCent/r-popgen-hackathon>) - provides functions  
95 for detecting outliers in multivariate space alongside procedures to manipulate,  
96 summarize, and visualize these data. The R software environment (R Core Team 2015)  
97 is free, open-source, and hosts a large collection of tools for statistical analysis, making

98 it the ideal host for the development and uptake of such a platform. Furthermore,  
99 because data visualization is an important part of verifying and identifying outliers, the  
100 R Shiny and Shiny Dashboard environments (Chang 2015; Chang et al. 2016) have been  
101 employed to provide MINOTAUR users with an interactive interface that streamlines  
102 the process of data input, statistical analysis, and graphical exploration. Together, these  
103 tools have the potential to increase the efficiency with which the results of genome  
104 scans are interrogated.

### 105 **Approaches to identifying multivariate outliers**

106 In the MINOTAUR package we implement four composite measures that can be used to  
107 integrate information over multiple univariate statistics: the Mahalanobis distance,  
108 harmonic mean distance, nearest neighbor distance, and kernel density deviance. We  
109 developed the latter three measures, which are related to Mahalanobis distance but  
110 make no strong assumptions about the parametric form of the data, meaning they can  
111 be applied to multivariate statistics that have complex correlated or even multimodal  
112 distributions. Some of these measures are heavily influenced by the distance of points  
113 from the multivariate centroid (Mahalanobis and harmonic mean distance) while others  
114 are mainly influenced by the sparseness of points in the local vicinity (nearest neighbor  
115 distance and kernel density deviance), and so we would expect the measures to behave  
116 differently from one another, and to vary in their behavior depending on the data at  
117 hand.

118 The calculation of these composite measures has been optimized for genome-scale data  
119 by using precompiled routines, written in C++ and integrated into R using the package  
120 Rcpp (Eddelbuettel and Francois 2011; Eddelbuettel 2013). Several packages devoted

121 to multivariate statistics that may be appropriate for genome-scale data already exist in  
122 R (see Supplementary Table 1), and thus users are free to utilize both existing statistical  
123 methods and the more targeted functions included within the MINOTAUR package.

124 *Mahalanobis distance.* The Mahalanobis distance is a multidimensional measure of the  
125 number of standard deviations that a point lies from the mean of a distribution. The  
126 Mahalanobis distance of a  $d$ -dimensional observation  $x_i = (x_{i1}, x_{i2}, \dots, x_{id})^T$  from a  
127 distribution of  $N$  variables with mean  $\bar{x} = (\bar{x}_1, \bar{x}_2, \dots, \bar{x}_d)^T$  and covariance matrix  $S$  is  
128 defined as follows (Mahalanobis 1936):

$$129 \quad D_M(x_i) = \sqrt{(x_i - \bar{x})^T S^{-1} (x_i - \bar{x})} . \quad (1)$$

130 This distance differs from the ordinary Euclidean distance due to the correction for  
131 covariance among observations, making it a better distance measure for genome scan  
132 summary statistics because it does not assume that statistics are independent (i.e.,  
133 Euclidean distance equals Mahalanobis distance when  $S$  is a diagonal matrix). However,  
134 this distance does make the assumption that points disperse smoothly from a single  
135 multivariate centroid, and so it will tend to perform poorly when observations have a  
136 complex or multimodal distribution.

137 *Harmonic mean distance.* In this context the “harmonic mean distance” of an  
138 observation  $x_i$  refers to the harmonic mean of the distances between this point and all  
139 other points. The distance measure used here is the Euclidian distance normalized by  
140 multiplying by the inverse covariance matrix. This ensures that results are not  
141 dominated by a few statistics with a large spread, and also accounts for any potential  
142 correlation between statistics, analogously to the Mahalanobis distance. Mathematically  
143 we can define the harmonic mean distance as follows:

144 
$$D_H(x_i) = N \left[ \sum_{j \neq i} [(x_i - x_j)S^{-1}(x_i - x_j)]^{-1/2} \right]^{-1} . \quad (2)$$

145 The harmonic mean is heavily influenced by small values, which in this context means  
146 local effects are amplified. However, more distant points also have some effect on the  
147 final value (unlike the nearest neighbor distance described below), and so the harmonic  
148 mean strikes a balance between local and global effects. This has some advantages in  
149 outlier detection, as observations that are both distant from the main mass of the data  
150 and have few neighbors in the local vicinity will tend to be outliers.

151 *Nearest neighbor distance.* The nearest neighbor distance of the observation  $x_i$  gives the  
152 minimum distance between this point and any other point. As with the harmonic mean  
153 distance, we use the Euclidian distance normalized by the inverse covariance matrix.  
154 Mathematically we can write

155 
$$D_N(x_i) = \min_{j \neq i} \left( \sqrt{(x_i - x_j)S^{-1}(x_i - x_j)} \right) . \quad (3)$$

156 This statistic exclusively measures local effects, being largest when an observation is a  
157 long way from any other point. Because this distance is only based on two points (the  
158 focal point and its nearest neighbor), it is not influenced by the global distribution of the  
159 data, unlike the harmonic mean distance.

160 *Kernel density deviance.* Kernel density-based methods attempt to capture  
161 mathematically the distribution of the data as the sum of a number of simple parametric  
162 distributions. Here we apply these methods to identifying multivariate outliers, defined  
163 as those points with a low density of data around them in multivariate space. We  
164 assume a multivariate normal kernel  $G(x_i | x_j, \lambda^2 S)$  centered at the point  $x_j$ , where  $\lambda$  is

165 the bandwidth of the kernel, which is scaled in each dimension by the covariance matrix  
166 of the data. We then calculate the leave-one-out log-likelihood (Leiva-Murillo and Artés-  
167 Rodríguez, 2012) of the point  $x_i$  as follows:

$$168 \quad L(x_i | \lambda) = \log\left(\frac{1}{N-1} \sum_{j \neq i} G(x_i | x_j, \lambda^2 S)\right) . \quad (4)$$

169 In other words, this is equal to the log-probability density of the point  $x_i$  under the  
170 kernel density distribution constructed from all points *apart from*  $x_i$ . Our final density-  
171 based measure is defined as follows:

$$172 \quad D_K(x_i) = -2L(x_i | \lambda) , \quad (5)$$

173 which is sometimes referred to as the Bayesian deviance. This will be large whenever  
174 the density of the point  $x_i$  is low, and so the kernel density deviance can be thought of as  
175 a measure of the sparseness of points around the focal point.

176 One challenge when using kernel density methods is choosing an appropriate value for  
177 the bandwidth. Here we simply use the bandwidth for which the total deviance of all  
178 points is minimized, i.e.

$$179 \quad \lambda^* = \operatorname{argmin}_{\lambda} \left( \sum_{i=1}^N -2L(x_i | \lambda) \right) . \quad (6)$$

180 It can be shown that this is equivalent to the maximum-likelihood value of  $\lambda$  under the  
181 leave-one-out criterion. The value  $\lambda^*$  can be found using the MINOTAUR function  
182 `kernelDeviance()`, which takes a vector of bandwidths as input and returns the total  
183 deviance of each. This function can be used to search for the minimum value of  $\lambda$   
184 manually, or via an optimization routine such as `optim()`. Users are also free to use any  
185 other bandwidth, entered manually, or in the absence of a user-defined bandwidth a



186 simple method based on Silverman's rule is implemented as a default (this assumes that  
187 data is normally distributed, and is a simple function of the standard deviation of the  
188 samples (Silverman 1986)).

## 189 **The MINOTAUR R package - an R Shiny graphical user interface for multivariate** 190 **outlier analysis and visualization**

191 The MINOTAUR package performs two main functions: (1) it calculates the compound  
192 multivariate outlier statistics described above and (2) it enables users to harness the  
193 interactive graphical power of the R Shiny environment to manipulate and visualize  
194 their data within the MINOTAUR graphical user interface (GUI). The GUI allows users to  
195 perform the former task with the click of a button; however, outlier identification can  
196 also be performed on the R command line using stand-alone functions available in  
197 MINOTAUR, if preferred. Directions for downloading and installing the package can be  
198 found at the end of this manuscript.

199 The MINOTAUR GUI is designed to streamline the process of genomic data analysis and  
200 outlier identification, taking users from data input to graphical output within a single  
201 platform. Distinct panels are used for each stage of the analysis, including data input  
202 and filtering, outlier detection via the methods described above, and plotting results  
203 (e.g., histograms, scatterplots, and Manhattan plots). An overview of the MINOTAUR GUI  
204 workflow is show in Figure 1.

205 In the *Data* panel, the MINOTAUR GUI allows users to either upload their own datasets  
206 or select among a set of four in-built example datasets. Data can be uploaded in a  
207 number of file formats, including comma- or tab-separated text files, and Rdata.  
208 Regardless of the file format, MINOTAUR expects all incoming datasets to be arranged in

209 data frames, with each row representing a different genetic locus and each column  
210 representing a different univariate genome scan statistic (e.g.,  $F_{st}$ , Tajima's  $D$ , etc.) or  
211 other piece of locus-specific metadata (e.g., SNP identifiers, chromosomes/scaffolds and  
212 positions, etc.). Raw data objects can be filtered within the GUI, meaning, for example,  
213 that columns not related to outlier analysis can be dropped at an early stage.

214 Four example datasets are made available to users within the MINOTAUR package and  
215 GUI. The "HumanGWAS" dataset contains example output from an unpublished human  
216 Genome-Wide Association Study. The simulated "NonParametricInverse" and  
217 "NonParametricMultimodal" datasets each contain an example of nonparametric data,  
218 one with an inverse relationship (Figure 3) and one that is highly multimodal  
219 (Supplemental Figure S1). The "TwoRefSim" dataset contains population genetic data  
220 simulated under a model of expansion from two refugia (Lotterhos and Whitlock 2015).  
221 Note that the example datasets can also be accessed outside the GUI by running the  
222 `data()` command with the appropriate dataset name. For example, to load the  
223 "HumanGWAS" dataset, type `data(HumanGWAS)` and hit ENTER. To learn more about a  
224 dataset while in the R terminal, add a question mark before the dataset name to load the  
225 relevant Help page; for example, type `?HumanGWAS` and hit ENTER.

226 In the *Outlier Detection* panel, multiple univariate statistics can be integrated to produce  
227 the compound distance measures described above. These measures can be appended to  
228 the data frame and visualized interactively in the *Produce Plots* panel, which includes  
229 several submenus with useful plots for visualizing high-dimensional datasets, including  
230 Manhattan plots, 1D histograms and density-based 2D Scatterplots. The plotting  
231 methods are designed with large genomic datasets in mind; for example the `plot2d()`  
232 function included with the package calculates the density of points for a given bin size

233 and shades bins according to the density of points within them, and then optionally  
234 adds user-supplied points (ideally a small subset of points, for example the outliers  
235 only) to the plot. Additional options allow users to log-scale statistics and control  
236 various other visual settings commonly used when plotting data in R (Figure 2).

### 237 **Example applications of multivariate outliers**

238 *Evaluation of computational speed.* First, we evaluated the speed of calculating the four  
239 compound distance measures for datasets with increasing numbers of loci (rows) and  
240 univariate statistics (columns). For this example, variables were randomly generated  
241 from a multivariate normal distribution. Table 1 gives the “order” of complexity of these  
242 algorithms, together with measured run-times for a dataset composed of 50,000 loci  
243 and 10 variables (see Supplementary Table S2 for extended run-time analyses). Overall,  
244 the Mahalanobis distance is calculated in a matter of seconds, even with particularly  
245 large datasets. The harmonic mean distance, nearest neighbor distance, and kernel  
246 density deviance each scale approximately equally with increasing dataset sizes, though  
247 the maximum likelihood estimate of the ideal bandwidth for the latter measure can add  
248 significant computation time.

249 *Example on simulated nonparametric distributions.* Some kinds of genomic data - for  
250 example gene expression data - may generate complex nonparametric distributions.  
251 Genes that have high expression in one environment may have low expression in  
252 another environment, while investigators may be interested in identifying genes that  
253 have moderate expression in both environments. To test the performance of the  
254 multivariate outlier statistics in nonparametric situations, we simulated two examples  
255 of nonparametric distributions.

256 In the first example, we simulated a distribution of two variables that follow an inverse  
257 relationship, with some additional noise. We used contour plots to visualize the  
258 different ways in which each of the compound distance measures changes over the two-  
259 dimensional plane (Figure 3). In these plots, the darker red lines indicate less-  
260 significant values of the test statistic and lighter yellow lines indicate more-significant  
261 values of the test statistic. We also looked at two manually chosen points on the plane -  
262 indicated by a blue square and triangle - chosen to represent different sorts of outliers.  
263 The blue triangle would not be considered an outlier from the perspective of either one-  
264 dimensional distribution despite being a clear outlier from the two-dimensional  
265 distribution, while the blue square would be considered an outlier in the first dimension  
266 but not the second. In this example, the nonparametric distribution affects the relative  
267 ability of the four statistics to identify each of these outliers (Figure 4). The blue triangle  
268 would not have the largest value (i.e., not be the most outlying point) by the  
269 Mahalanobis or the harmonic mean distance, while it would have the largest value by  
270 nearest neighbor distance or kernel density deviance. In contrast, the blue square has  
271 the largest value of the test statistic by all four methods.

272 In the second example, we simulated a highly multimodal distribution from a normal  
273 mixture model. In this example, it can be seen how the parametric assumption of the  
274 Mahalanobis distance fails to capture the complexity of the data (Supplementary Figure  
275 S1). In contrast to the previous example, the harmonic mean distance behaves similarly  
276 to the kernel density deviance, and nearest neighbor distance has the most complex  
277 contour landscape.

278 *Example on simulated genomic data.* To test the power of multivariate statistics for  
279 genome scans, we applied them to a published simulated dataset that was used to test

280 different genome scan methods (Lotterhos and Whitlock 2014, 2015). Briefly, a  
281 landscape simulator was used to simulate haploid neutral and selected loci that adapted  
282 to an environmental cline (Lotterhos and Whitlock 2015). The landscape consisted of  
283 360 x 360 demes and the allele frequency of each deme changed each generation  
284 according to recurrence equations for mutation, migration, selection (if applicable), and  
285 drift (Lotterhos and Whitlock 2015). For the dataset used in this example, a total of  
286 9900 neutral and 100 selected loci (simulated under varying strengths of selection: 12  
287 loci with  $s = 0.1$ , 38 loci with  $s = 0.01$ , and 50 loci with  $s = 0.005$ ) were simulated under  
288 a two-refuge demographic expansion. Individuals were then sampled from the  
289 landscape according to the allele frequency in each deme at 30 randomly chosen  
290 locations on the landscape at 20 individuals per location. For additional details see  
291 Lotterhos and Whitlock (2014, 2015).

292 The simulated data were used to create a single nucleotide polymorphism (SNP) table  
293 and this data was used to perform genome scans in the programs Bayenv2 (Günther  
294 and Coop 2013) and LFMM (Frichot et al. 2013, now implemented in the R package LEA:  
295 Frichot and François 2015). A total of four univariate statistics from these two  
296 programs were used in the search for multivariate outliers: (i) log-Bayes Factor (log-BF,  
297 a measure of the association between allele frequency and the environment in  
298 Bayenv2), (ii) Spearman's rho (a measure of the association between allele frequency  
299 and the environment in Bayenv2), (iii)  $X^T X$  (a measure of genetic differentiation among  
300 populations in Bayenv2), and (iv) Z-score (a measure of the association between  
301 genotype and the environment in LFMM). These four univariate statistics, plotted in  
302 Figure 4, were previously shown to have different strengths and weaknesses depending  
303 on sampling design and demographic history (Lotterhos and Whitlock 2015).

304 To illustrate the flexibility of the outlier functions implemented in MINOTAUR, we  
305 calculated multivariate outliers in two ways, corresponding to two different ways of  
306 calculating the covariance matrix  $S$  in equations (1) to (4). First, we used the traditional  
307 method of calculating the covariance matrix based on all the data. For high-dimensional  
308 data, estimation of the multivariate mean and covariance (location and scatter) are  
309 expected to be robust to outliers as long as the proportion of outliers in the data is less  
310 than  $1/(k+1)$ , where  $k$  is the number variables in the dataframe (Ro et al. 2015).  
311 However, we found that even in this small dataframe of only 4 variables and 10,000 loci,  
312 the 1% of selected loci (a fraction of which were true outliers) affected the estimation of  
313 the covariance matrix. For this reason, our MINOTAUR functions are designed to allow  
314 the user to input their own covariance matrix. To illustrate this use of the function, we  
315 also calculated a robust multivariate location and scatter estimate with a high  
316 breakdown point, using the 'Fast MCD' (Minimum Covariance Determinant) estimator  
317 with the function `CovNAMcd` in the R package `rrcovNA` (Rousseeuw et al 1999; Todorov  
318 et al. 2011).

319 To compare the ability of the univariate statistics and the multivariate statistics to  
320 separate neutral from selected loci, we calculated the empirical power. The empirical  
321 power is based on using all known neutral loci to generate a null distribution, and then  
322 for each locus an empirical  $p$ -value is calculated based on its cumulative frequency in  
323 this null distribution. To control for false discovery rate, empirical  $p$ -values were  
324 converted to  $q$ -values (in the R package `qvalue`: Dabney and Storey 2014) and loci with  
325 a  $q$ -value less than 0.05 were retained as positive hits (a  $q$ -value of 0.05 has a desired  
326 rate of 5 false positives out of 100 positive hits).

327 For the univariate statistics, the empirical power was highest for log-BF (0.54) and  
328 lowest for Z-score (0.15), with Spearman's rho (0.46) and  $X^T X$  (0.42) also showing  
329 moderate power. For the multivariate statistics with the default covariance estimation,  
330 the empirical power was high for harmonic mean distance and Mahalanobis distance  
331 (0.41 for both), with kernel density and nearest neighbor distance performing poorly in  
332 this case (0.09 for both) (Supplementary Figure S2). For the user-input covariance  
333 matrix estimated with a high breakdown point (i.e., less influenced by outliers), the  
334 empirical power was highest for harmonic mean distance and Mahalanobis distance  
335 (0.58 for both), with kernel density and nearest neighbor distance still performing  
336 poorly (Figure 5). This final example illustrates the potential of Mahalanobis and  
337 harmonic mean distance to improve the signal-to-noise ratio in genome scans, because  
338 the empirical power in this case was higher than any univariate statistic alone.

### 339 **Discussion**

340 Although the number of packages for population genetic data analysis in the R software  
341 is rapidly increasing (<http://popgen.nescent.org/PACKAGES.html>), basic tools for  
342 manipulating and visualizing genome-scale datasets have so far been lacking.

343 MINOTAUR fills this gap using the R Shiny Dashboard package to implement a GUI that  
344 makes it easy to upload, manipulate, analyze, and visualize genomic data.

345 The multivariate metrics calculated in MINOTAUR contribute to a growing number of  
346 multivariate tools implemented in the R environment (see Supplementary Table S1).

347 Methods that are influenced heavily by the distance of a point from the centroid in  
348 multivariate space (such as Mahalanobis and the harmonic mean distance) will perform  
349 differently compared with methods that are influenced mainly by the sparseness of

350 points in multivariate space (such as nearest neighbor distance and kernel density), as  
351 illustrated in the examples here. However, depending on how the data are distributed,  
352 the harmonic mean distance may be influenced by both these factors. For a single  
353 simulated dataset, we found that robust use of the Mahalanobis or harmonic mean  
354 distance (i.e., when the covariance matrix used was estimated with a high breakdown  
355 point) could have higher power than any single univariate statistic alone. Although  
356 nearest neighbor distance and kernel density deviance performed poorly on the  
357 simulated genomic data, they may be useful in application to other kinds of  
358 nonparametric data, as illustrated in our examples (Figures 3 and S1). Further  
359 evaluation, however, will be needed on both simulated and empirical data to determine  
360 whether multivariate outlier approaches will improve the signal-to-noise ratio in  
361 genome scans.

362 The MINOTAUR package is designed to complement existing tools for the analysis and  
363 integration of genome-scan data. Thus, in addition to providing its own tools for  
364 genome-scale analyses, MINOTAUR can serve as a platform for the further analysis and  
365 visualization of results generated by other R packages. Examples include results from  
366 differential gene expression (LIMMA: Ritchie et al. 2015; DESeq: Anders and Huber  
367 2010; SeqGSEA: Wang and Cairns 2014), outliers for genetic differentiation (OutFLANK:  
368 Whitlock and Lotterhos 2015; PCAdapt: Luu and Blum 2015), genetic-environment  
369 associations (LEA: Frichot and François 2015), or genome-wide association studies (e.g.  
370 GenABEL: Aulchenko et al. 2007; BlueSNP: Huang et al. 2013).

371 Recent developments such as the R Shiny and Shiny Dashboard environments (Chang  
372 2015; Chang et al. 2016) dramatically aid in the development of R-based user-friendly  
373 web interfaces. Taking advantage of these tools, MINOTAUR is able to offer a new



374 platform for visualizing and integrating genomic data that may appeal to molecular  
375 ecologists, modellers, statisticians, and public health agencies.

## 376 **Resources**

377 **Availability:** Upon acceptance for publication, MINOTAUR will be distributed on CRAN  
378 (<http://cran.r-project.org/>) and be available for R on Windows, Mac OSX, and Linux  
379 platforms. Currently, MINOTAUR can be accessed via the following steps:

```
380 • install.packages("devtools", dependencies=TRUE)  
381 • library(devtools)  
382 • install_github("NESCent/MINOTAUR", build_vignettes=TRUE)  
383 • library(MINOTAUR)  
384 • MINOTAUR()
```

385 Note to reviewers: If you are facing issues with installation, try updating to the newest  
386 version of R and reinstalling devtools from source. MINOTAUR has been tested on R  
387 version 3.3.0.

388 **Licence:** GNU General Public Licence (GPL) >= 2.

389 **Documentation:** Besides the usual package documentation, MINOTAUR is released  
390 with a tutorial which can be opened by typing: `vignette("MINOTAUR")`.

391 **Development:** The development of MINOTAUR is hosted on GitHub:  
392 (<https://github.com/NESCent/MINOTAUR>).

## 393 394 **Acknowledgments**

395 The resource reported in this paper began at the Population Genetics in R Hackathon,  
396 which was held in March 2015 at the National Evolutionary Synthesis Center (NESCent)  
397 in Durham, NC, with the goal of addressing interoperability, scalability, and workflow  
398 building challenges for the population genetics package ecosystem in R. The authors  
399 were participants in the hackathon, and are indebted to NESCent (NSF #EF-0905606)  
400 for hosting and supporting the event. RV, CC, DCC, SMS benefited from travel support to  
401 attend this Hackathon.

## 402 **Author Contributions**

403 RV and KEL conceptualized the study. RV derived the compound outlier measures and  
404 implemented them in R. RV and CC conceptualized and implemented the Shiny  
405 Dashboard GUI. CC managed R package development, package structure and  
406 documentation. All authors contributed R code for plotting in the Shiny Dashboard. DCC  
407 wrote the vignette for the package and estimated function computational time. KEL  
408 performed analysis of the performance of compound measures on simulated data. All  
409 authors contributed to writing this manuscript.

## 410 **References**

- 411 Allendorf FW, Hohenlohe PA, Luikart G (2010) Genomics and the future of conservation  
412 genetics. *Nature Reviews Genetics*, **11**, 697–709.
- 413 Anders S, Huber W (2010) Differential expression analysis for sequence count data.  
414 *Genome Biology*, **11**, R106
- 415 Aulchenko YS, Ripke S, Isaacs A, Duijn CMV (2007) GenABEL: an R library for genome-  
416 wide association analysis. *Bioinformatics*, **23**, 1294–1296.
- 417 Brachi B, Morris GP, Borevitz JO (2011) Genome-wide association studies in plants: the  
418 missing heritability is in the field. *Genome Biology*, **12**, 232.
- 419 Carlson CS, Eberle MA, Kruglyak L, Nickerson DA (2004) Mapping complex disease loci  
420 in whole-genome association studies. *Nature*, **429**, 446–452.
- 421 Chang W (2015). shinydashboard: Create Dashboards with 'Shiny'. R package version  
422 0.5.1. <https://CRAN.R-project.org/package=shinydashboard>
- 423 Chang W, Cheng J, Allaire JJ, Xie Y, McPherson J (2016). shiny: Web Application  
424 Framework for R. R package version 0.13.1. [https://CRAN.R-](https://CRAN.R-project.org/package=shiny)  
425 [project.org/package=shiny](https://CRAN.R-project.org/package=shiny)
- 426 Dabney A, Storey JD (2014) qvalue: Q-value estimation for false discovery rate control.  
427 R package, version 1.38.0. <https://github.com/jdstorey/qvalue>.
- 428 De Mita S, Thuillet AC, Gay L *et al.* (2013) Detecting selection along environmental  
429 gradients: analysis of eight methods and their effectiveness for outbreeding and  
430 selfing populations. *Molecular Ecology*, **22**, 1383–1399.
- 431 De Villemereuil PD, Frichot É, Bazin É, François O, Gaggiotti OE (2014) Genome scan  
432 methods against more complex models: when and how much should we trust  
433 them? *Molecular Ecology*, **23**, 2006–2019.
- 434 Eddelbuettel D (2013) Seamless R and C++ Integration with Rcpp. Springer, New York.  
435 ISBN 978-1-4614-6867-7.
- 436 Eddelbuettel D, François R (2011) Rcpp : Seamless R and C Integration. *Journal of*  
437 *Statistical Software*, **40**, 1-18
- 438 Evangelou E, Ioannidis JP (2013) Meta-analysis methods for genome-wide association  
439 studies and beyond. *Nature Reviews Genetics*, **14**, 379–389.
- 440 Frichot E, François O (2015) LEA : An R package for landscape and ecological  
441 association studies. *Methods in Ecology and Evolution*, **6**, 925–929.

- 442 Frichot E, Schoville SD, Bouchard G, Francois O (2013) Testing for Associations between  
443 Loci and Environmental Gradients Using Latent Factor Mixed Models. *Molecular*  
444 *Biology and Evolution*, **30**, 1687–1699.
- 445 Funk WC, Mckay JK, Hohenlohe PA, Allendorf FW (2012) Harnessing genomics for  
446 delineating conservation units. *Trends in Ecology & Evolution*, **27**, 489–496.
- 447 Galesloot TE, van Steen K, Kiemeny LALM, Janss LL, Vermeulen SH (2014). A  
448 comparison of multivariate genome-wide association methods. *PLoS ONE*, **9**,  
449 e95923.
- 450 Goddard ME, Hayes BJ (2009) Mapping genes for complex traits in domestic animals  
451 and their use in breeding programmes. *Nature Reviews Genetics*, **10**, 381–391.
- 452 Hindorff LA, Sethupathy P, Junkins HA *et al.* (2009) Potential etiologic and functional  
453 implications of genome-wide association loci for human diseases and traits.  
454 *Proceedings of the National Academy of Sciences*, **106**, 9362–9367.
- 455 Hoban S, Kelley JK, Lotterhos KE, Bradburd G, Lowry DB, Poss ML, Reed LK, Storfer A,  
456 Whitlock MC (2016) Finding the genetic basis of local adaptation: problems,  
457 pitfalls, and future direction. *American Naturalist* (In revision)
- 458 Hohenlohe PA, Phillips PC, Cresko WA (2010) Using population genomics to detect  
459 selection in natural populations: key concepts and methodological considerations.  
460 *International Journal of Plant Sciences*, **171**, 1059–1071.
- 461 Huang H, Tata S, Prill RJ (2012) BlueSNP: R package for highly scalable genome-wide  
462 association studies using Hadoop clusters. *Bioinformatics*, **29**, 135–136.
- 463 Kohn MH, Murphy WJ, Ostrander EA, Wayne RK (2006) Genomics and conservation  
464 genetics. *Trends in Ecology & Evolution*, **21**, 629–637.
- 465 Leiva-Murillo JM, Artés-Rodríguez A (2012) Algorithms for maximum-likelihood  
466 bandwidth selection in kernel density estimators. *Pattern Recognition Letters*, **33**,  
467 1717–1724.
- 468 Lotterhos KE, Francois O, Blum M (2016) Not just methods: User expertise explains the  
469 variability of outcomes of genome-wide studies. *Molecular Ecology* (In review).
- 470 Lotterhos KE, Whitlock MC (2014) Evaluation of demographic history and neutral  
471 parameterization on the performance of F<sub>ST</sub> outlier tests. *Molecular Ecology*, **23**,  
472 2178–2192.
- 473 Lotterhos KE, Whitlock MC (2015) The relative power of genome scans to detect local  
474 adaptation depends on sampling design and statistical method. *Molecular Ecology*,  
475 **24**, 1031–1046.
- 476 Luu K, Blum MGB (2015). pcadapt: Principal Component Analysis for Outlier Detection.  
477 R package version 2.1. <https://CRAN.R-project.org/package=pcadapt>
- 478 Mahalanobis PC (1936) On the generalised distance in statistics. *Proceedings of the*  
479 *National Institute of Sciences of India*, **2**, 49–55.
- 480 Mccarthy MI, Abecasis GR, Cardon LR *et al.* (2008) Genome-wide association studies for  
481 complex traits: consensus, uncertainty and challenges. *Nature Reviews Genetics*, **9**,  
482 356–369.
- 483 Mccarthy MI, Hirschhorn JN (2008) Genome-wide association studies: past, present and  
484 future. *Human Molecular Genetics*, **17**, R100–101.
- 485 O'Reilly, P. F. *et al.* MultiPhen: joint model of multiple phenotypes can increase  
486 discovery in GWAS. *PLoS One* **7**, e34861 (2012).
- 487 Patterson, N., Price, A. L. & Reich, D. Population structure and eigenanalysis. *PLoS Genet.*  
488 **2**, e190 (2006).
- 489 R Core Team (2015) R: A language and environment for statistical computing. R  
490 Foundation for Statistical Computing, Vienna, Austria. <https://www.R-project.org/>.

- 491 Rellstab C, Gugerli F, Eckert AJ, Hancock AM, Holderegger R (2015) A practical guide to  
492 environmental association analysis in landscape genomics. *Molecular Ecology*, **24**,  
493 4348–4370.
- 494 Ritchie ME, Phipson B, Wu D *et al.* (2015) limma powers differential expression  
495 analyses for RNA-sequencing and microarray studies. *Nucleic Acids Research*, **43**, 1-  
496 13.
- 497 Rousseeuw PJ, Driessen KV (1999) A Fast Algorithm for the Minimum Covariance  
498 Determinant Estimator. *Technometrics*, **41**, 212–223.
- 499 Savolainen O, Lascoux M, Merilä J (2013) Ecological genomics of local adaptation.  
500 *Nature Reviews Genetics*, **14**, 807–820.
- 501 Silverman BW (1986) *Density estimation for statistics and data analysis*. Chapman and  
502 Hall, London.
- 503 Tiffin P, Ross-Ibarra J (2014) Advances and limits of using population genetics to  
504 understand local adaptation. *Trends in Ecology & Evolution*, **29**, 673–680.
- 505 Todorov V, Templ M, Filzmoser P (2011) Detection of multivariate outliers in business  
506 survey data with incomplete information. *Advances in Data Analysis and*  
507 *Classification*, **5**, 37–56.
- 508 Varshney RK, Nayak SN, May GD, Jackson SA (2009) Next-generation sequencing  
509 technologies and their implications for crop genetics and breeding. *Trends in*  
510 *Biotechnology*, **27**, 522–530.
- 511 Vatsiou AI, Bazin E, Gaggiotti OE (2016) Detection of selective sweeps in structured  
512 populations: a comparison of recent methods. *Molecular Ecology*, **25**, 89–103.
- 513 Verity R, Nichols RA (2014) What is genetic differentiation, and how should we measure  
514 it-  $G_{ST}$ ,  $D$ , neither or both? *Molecular Ecology*, **23**, 4216–4225.
- 515 Wang X, Cairns MJ (2014) SeqGSEA: a Bioconductor package for gene set enrichment  
516 analysis of RNA-Seq data integrating differential expression and splicing.  
517 *Bioinformatics*, **30**, 1777–1779.
- 518 Wang Z, Gerstein M, Snyder M (2009) RNA-Seq: a revolutionary tool for transcriptomics.  
519 *Nature Reviews Genetics*, **10**, 57–63.
- 520 Whitlock MC, Lotterhos KE (2015) Reliable Detection of Loci Responsible for Local  
521 Adaptation: Inference of a Null Model through Trimming the Distribution of  $F_{ST}$ .  
522 *The American Naturalist*, **186**, S24–36.
- 523 Yang J, Benyamin B, Mcevoy BP *et al.* (2010) Common SNPs explain a large proportion  
524 of the heritability for human height. *Nature Genetics*, **42**, 565–569.

525 **Tables**

526 **Table 1.** Multivariate outlier detection methods implemented in MINOTAUR and  
527 associated computational run times. Computational complexity is given in “big O”  
528 notation, with  $N$  referring to the number of observations and  $k$  the number of statistics  
529 (dimensions). Run times were determined using an Apple iMac with a 3.1 GHz Intel  
530 Core i5 processor and 32 GB of RAM running Apple OSX 10.9.5 and R version 3.2.3. Note  
531 that for computation time the kernel density deviance includes both the maximum  
532 likelihood estimation of the optimal bandwidth and the density calculations based on  
533 the optimal bandwidth.

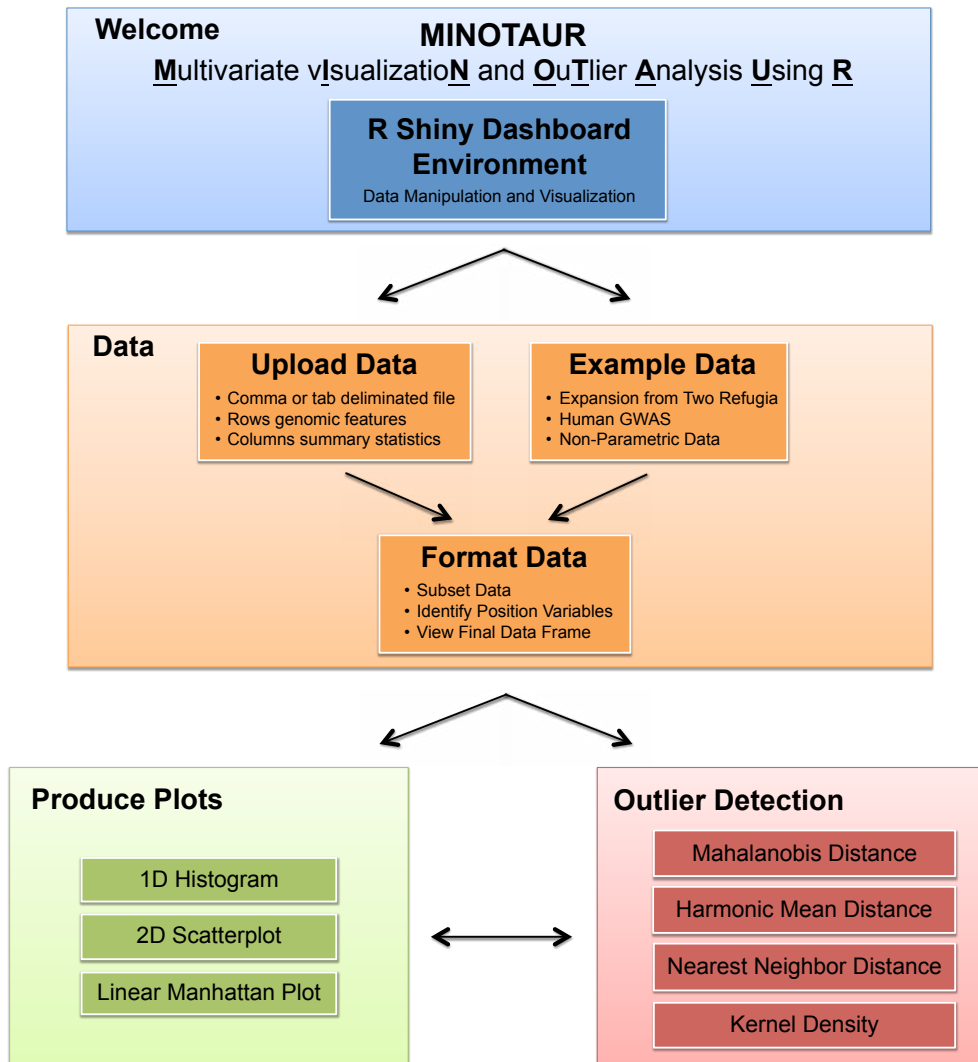
Compound measure	Description	R Function	Computational complexity (big O notation)	Computation Elapsed Time for 50,000 loci & 10 variables (hh:mm:ss.ms)
Mahalanobis distance	Distance from multivariate centroid	Mahalanobis()	$O(Nk^2)$	00:00:00.095
Harmonic mean distance	Inverse-weighted distance from all other points	harmonicDist()	$O(Nk^2)$	00:04:13.620
Kernel density deviance	Local density of points	kernelDist()	$O(Nk^2)$	01:40:03.600
Nearest neighbor distance	Distance to nearest neighbor	neighborDist()	$O(Nk^2)$	00:04:07.020

534

535

536 **Figures**

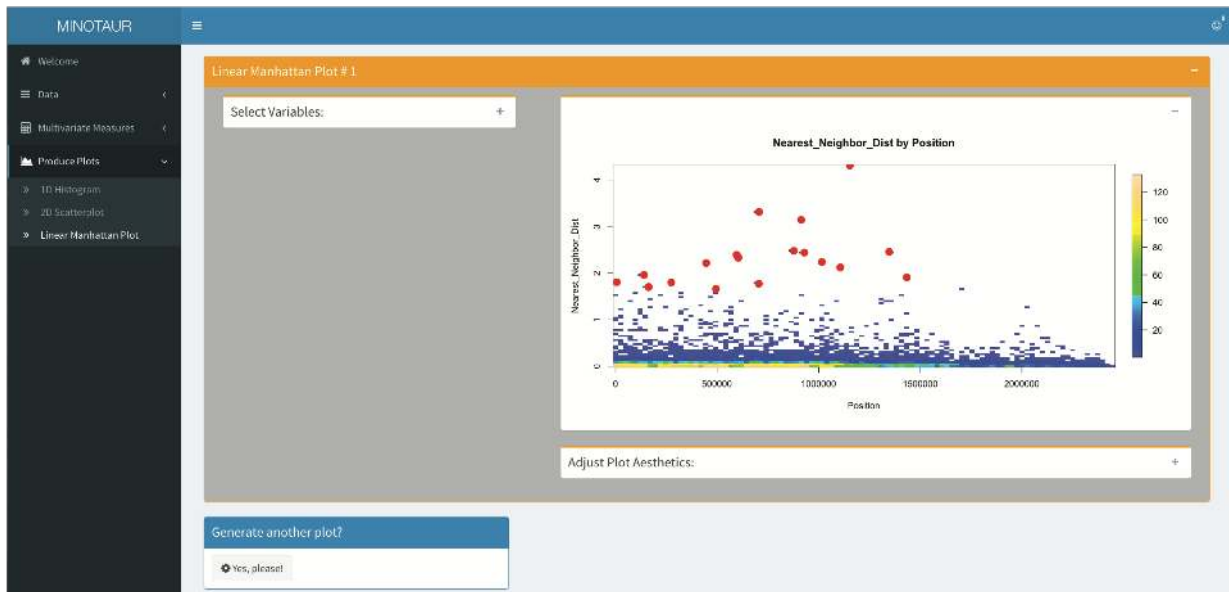
537 **Figure 1.** Graphical overview of the MINOTAUR GUI workflow.



538

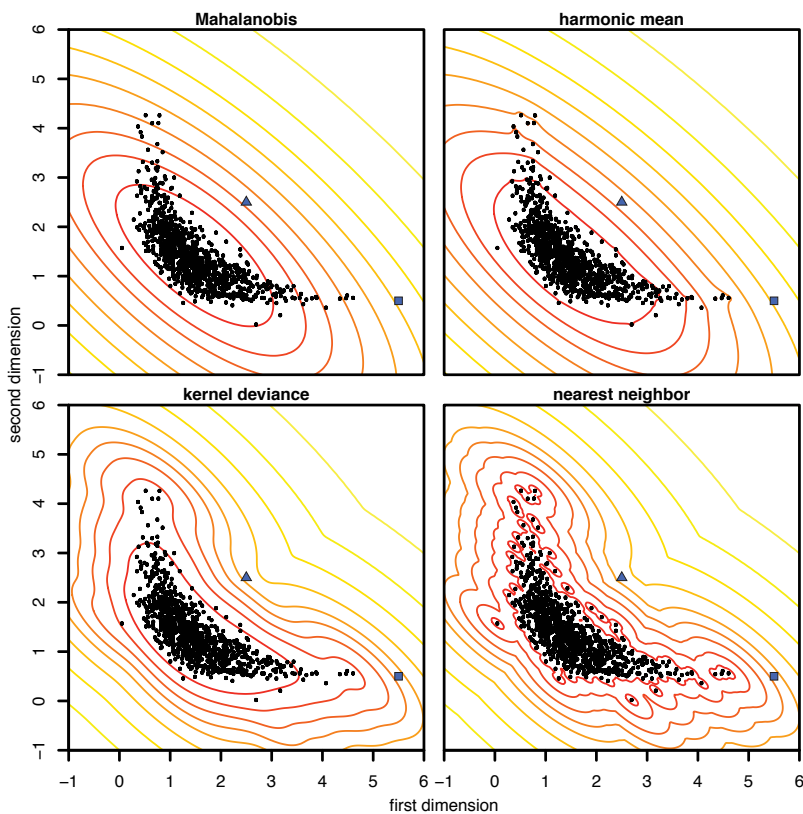
539

540 **Figure 2.** Screenshot of MINOTAUR GUI highlighting the overall interface and the ability  
541 to visualize multivariate distributions. The plot is a Manhattan plot of the nearest  
542 neighbor distance across loci for all traits in the “HumanGWAS” example dataset  
543 provided as part of MINOTAUR. The base scatter plot demonstrates the binned  
544 visualization, where the density of data in an area is apparent from the color. 99.5%  
545 percentile outliers are indicated with solid orange circles. Visualization menus have  
546 been collapsed to simplify the image. Additional plots can also be stacked below to  
547 enable comparisons across multiple plots (not shown).



549

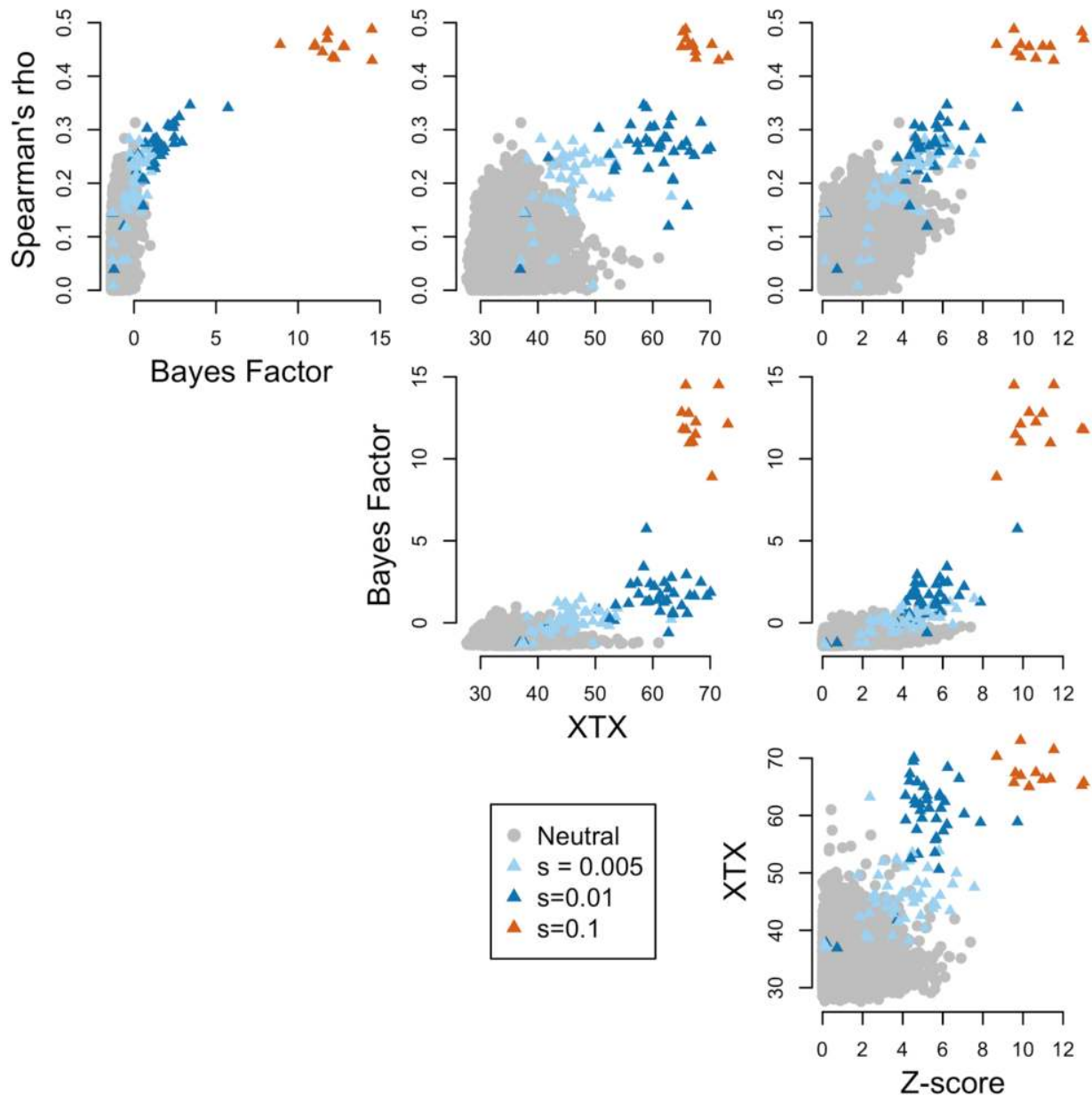
550 **Figure 3.** Comparison of multivariate distance measures for nonparametric example  
551 data. Black dots show the simulated data, in which the two statistics (dimensions) are  
552 assumed to follow an inverse relationship with some additional noise. Solid lines show  
553 the distance measure computed at each point in the plane, arranged in 10% quantiles  
554 (e.g. the inner ring shows the 10% of locations with the smallest distance). The blue  
555 square and triangle show particular outlier points referred to in the main text.



556

557

558 **Figure 4.** Distributions of four univariate statistics from the two refuge dataset from  
559 Lotterhos and Whitlock (2015).

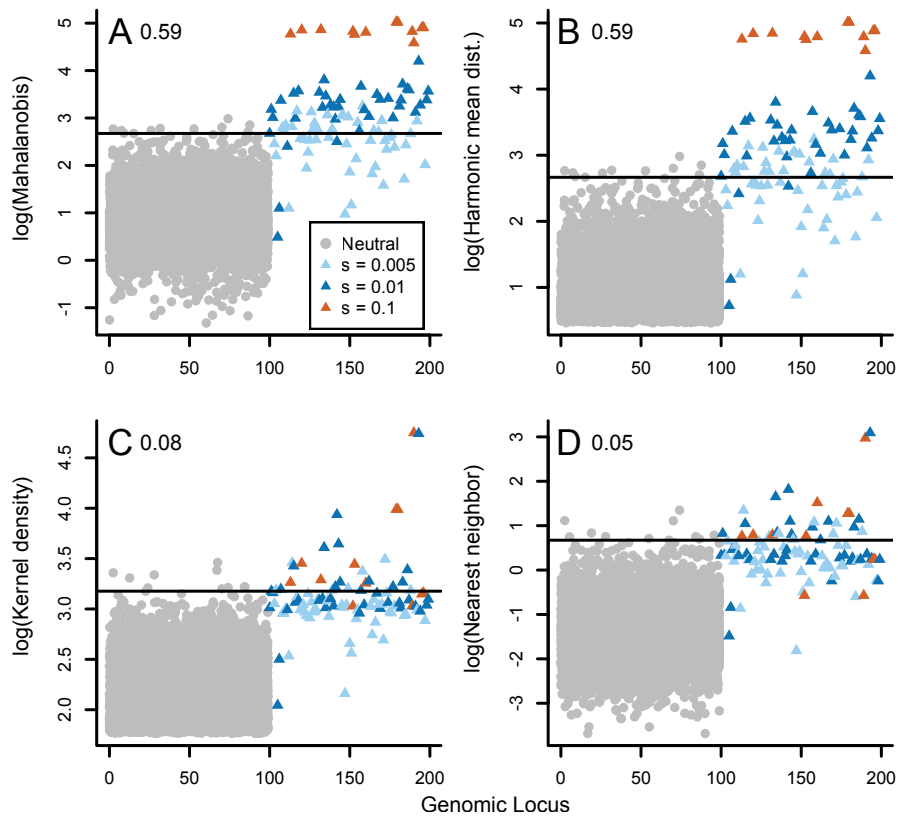


560

561

562 **Figure 5.** Distributions of the four multivariate compound statistics applied to the four  
563 univariate statistics shown in Figure 2. The MCD calculation of the covariance matrix  
564 was used. All 9900 neutral loci are plotted on indexes 0-100, and the selected loci are  
565 plotted on indexes 100-200. Note log transformation of each variable on the y-axis for:  
566 A) Mahalanobis distance, B) Harmonic mean distance, C) Kernel density, and D) Nearest  
567 Neighbor distance. The empirical power of the statistic to discriminate neutral from  
568 selected loci (see main text for details) is shown in the upper left hand corner.





## Supplementary Material for the Paper *MINOTAUR: A platform for the analysis and visualization of multivariate results from genome scans with R Shiny*

**Table S1.** Table of multivariate outlier statistics in other R packages that could be used in the context of genomic scans.

**Supplementary Table S1.** Table of multivariate outlier statistics available in other R packages

Multivariate Outlier Statistic	R Package	R Function	Brief Description	Reference
Hierarchical Clustering Ranks	DMwR	outliers.ranking()	Uses an agglomerative hierarchical clustering algorithm to rank outlierness.	Torgo 2011
Projection Congruent Subset	FastPCS	FastPCS()	Computes fast and robust multivariate outlyingness index.	Vakili & Schmitt 2014
Kernel Density Estimator	ks	kde()	Computes the kernel density estimate for up to 6 dimensional datasets.	Duong 2007
Mahalanobis Distance	mvoutlier	locoutNeighbor()	Computes global and pairwise Mahalanobis distances for outlier visualization with number of neighbors varying and fraction of neighbors fixed.	Filzmoser & Gschwandtner 2015
Mahalanobis Distance	mvoutlier	locoutSort()	Computes global and pairwise Mahalanobis distances for interactive outlier visualization.	''
Mahalanobis Distance	mvoutlier	locoutPercent()	Computes global and pairwise Mahalanobis distances for outlier visualization with number of neighbors fixed and varying fraction of neighbors.	''
Principal Components Distance	mvoutlier	pcout()	Principal components distances are used to identify weighted location and scatter of outliers.	''
Mahalanobis Distance	mvoutlier	sign1()	Principal components are used to calculate Mahalanobis distance covariance matrix and a critical value cutoff is used to determine outliers from chi-squared distribution.	''
Principal Components Distance	mvoutlier	sign2()	Principal components distances are computed and transformed to approach a chi-squared distribution and a critical value cutoff is used to detect outlier.	''
Adjusted Mahalanobis Distance	mvoutlier	arw()	Adjusts outlier rejection thresholds by using an adaptive reweighting estimator and determines outliers by the supremum of the difference between Mahalanobis distance and the theoretical distribution function.	''

**Supplementary Table S1.** Table of multivariate outlier statistics available in other R packages

Multivariate Outlier Statistic	R Package	R Function	Brief Description	Reference
Mahalanobis Distance	rrcovHD	OutlierMahdist()	Calculates Mahalanobis distance and determines outliers based on a critical value of the chi-squared distribution.	Todorov 2016
Mahalanobis Distance	CerioliOutlierDetection	cerioli2010.fsmcd.test()	Calculates Mahalanobis distance based on the finite-sample reweighted Minimum Covariance Determinant (MCD) dispersion estimate.	Cerioli 2010
Mahalanobis Distance	CerioliOutlierDetection	cerioli2010.irmcd.test()	Calculates Mahalanobis distances based on an iterated reweighted MCD dispersion estimate.	''
Mahalanobis Distance & Adjusted Mahalanobis Distance	MVN	mvOutlier()	Calculates Mahalanobis distance or adjusted Mahalanobis distance and determines outliers based on the 97.5 percent quantile critical value of the chi-square distribution.	Korkmaz, Goksuluk & Zararsiz 2015

**References:**

- Cerioli A (2010) Multivariate Outlier Detection With High-Breakdown Estimators. *Journal of the American Statistical Association*, **105**, 147–156.
- Duong T (2007) ks: Kernel Density Estimation and Kernel Discriminant Analysis for Multivariate Data in R. *Journal of Statistical Software*, **21**, 1–16.
- Filzmoser P, Gschwandtner M (2015) Mvoutlier: Multivariate Outlier Detection Based on Robust Methods. R package version 2.0.6. <https://cran.r-project.org/web/packages/mvoutlier/mvoutlier.pdf>
- Korkmaz S, Goksuluk D, Zararsiz G (2014) MVN: an R package for assessing multivariate normality. *R Journal*, **6**, 151-162.
- Todorov V (2016) Robust Multivariate Methods for high Dimensional Data. R package version 0.2-4. <https://cran.r-project.org/web/packages/rrcovHD/rrcovHD.pdf>
- Torgo L (2011) *Data mining with R: learning with case studies*. Chapman & Hall/CRC, Boca Raton.
- Vakili K, Schmitt E (2014) Finding multivariate outliers with FastPCS. *Computational Statistics & Data Analysis*, **69**, 54–66.

**Table S2.** Computation times for the four multivariate outlier detection methods in MINOTAUR for datasets up to 100,000 loci (rows) and 20 variables (columns) in hh:mm:ss.ms format. Run times were determined using an Apple iMac with a 3.1 GHz Intel Core i5 processor and 32 GB of RAM running Apple OSX 10.9.5 and R version 3.2.3. Note that the kernel density deviance includes both the maximum likelihood estimation of the optimal bandwidth and the density calculations based on the optimal bandwidth.

No. Loci	No. Variables	Mahalanobis distance	Harmonic mean distance	Kernel density deviance	Nearest neighbor distance
1000	5	00:00:00.001	00:00:00.040	00:00:01.233	00:00:00.034
1000	10	00:00:00.002	00:00:00.098	00:00:02.366	00:00:00.094
1000	15	00:00:00.003	00:00:00.188	00:00:04.303	00:00:00.185
1000	20	00:00:00.005	00:00:00.318	00:00:07.548	00:00:00.317
5000	5	00:00:00.003	00:00:00.986	00:00:30.215	00:00:00.829
5000	10	00:00:00.008	00:00:02.431	00:00:57.794	00:00:02.382
5000	15	00:00:00.014	00:00:04.809	00:01:49.900	00:00:04.622
5000	20	00:00:00.024	00:00:07.968	00:02:46.393	00:00:07.821
10000	5	00:00:00.006	00:00:03.922	00:02:00.694	00:00:03.328
10000	10	00:00:00.017	00:00:09.728	00:03:52.081	00:00:09.310
10000	15	00:00:00.169	00:00:18.773	00:06:53.011	00:00:18.487
10000	20	00:00:00.041	00:00:32.415	00:11:10.482	00:00:31.735
50000	5	00:00:00.045	00:01:37.808	00:50:19.078	00:01:24.120
50000	10	00:00:00.095	00:04:13.621	01:40:03.603	00:04:07.027
50000	15	00:00:00.161	00:09:12.221	00:19:36.847	00:08:51.240
50000	20	00:00:00.240	00:16:38.589	05:45:21.387	00:16:12.965
100000	5	00:00:00.085	00:06:35.265	03:21:34.758	00:05:35.996
100000	10	00:00:00.184	00:17:01.708	09:28:30.378	00:16:24.535
100000	15	00:00:00.324	00:36:19.473	13:28:52.158	00:37:20.698
100000	20	00:00:00.487	01:14:47.783	24:45:25.372	01:14:24.686

**Figure S1.** Comparison of multivariate distance measures for multi-modal example data. Black dots show the simulated data, drawn from a bivariate normal mixture model. Solid lines show the distance measure computed at each point in the plane, arranged in 10% quantiles, equivalently to Figure 3 in the main paper.

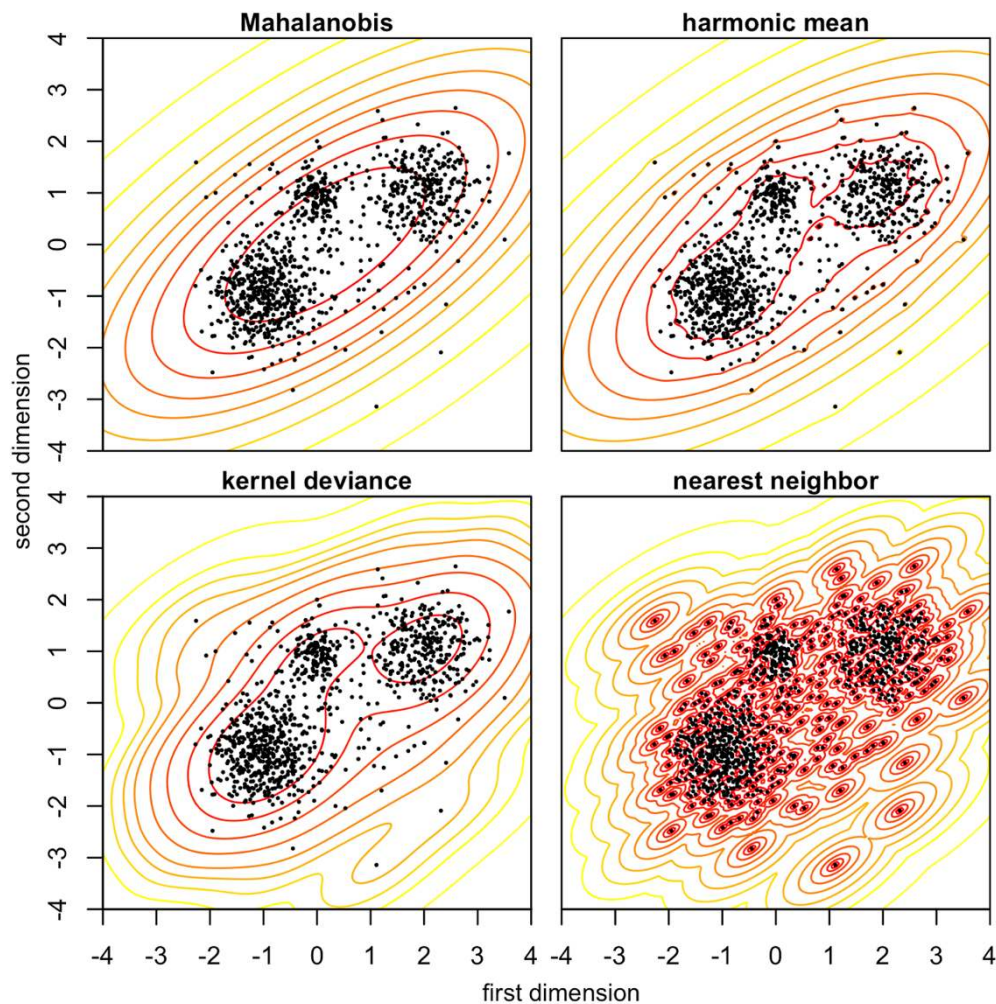


**Figure S2.** Analogue to Figure 5 in the main paper, but with a default estimate of covariance using all the data.

